

Three-Dimensional Localization of RF Emitters: A Semantic Segmentation-based Image Processing Approach

Huichao Chen*, Zheng Wang*, Wei Wang* and Guoru Ding[†]

*Key Laboratory of Dynamic Cognitive System of Electromagnetic Spectrum Space,
Ministry of Industry and Information Technology, Nanjing University of Aeronautics
and Astronautics, Nanjing, 210016, China

[†]College of Communications Engineering, Army Engineering University, Nanjing, 210007, China

Abstract—Localization is an important issue in wireless sensor networks (WSNs). Aimed at the shortcomings of low localization accuracy of the existing 3D localization algorithms, in this paper, we develop a three-dimensional localization scheme of RF emitters which combines collaborative spectrum sensing with deep learning. We propose a semantic segmentation approach to identify the coverage range of the RF emitters which converts the three-dimensional sensing data into a series of two-dimensional image slices. Then, we design a weighted localization algorithm to accurately locate the RF emitters. The simulation results show that the proposed method is accurate in positioning under various parameter configurations.

I. INTRODUCTION

WSNs are composed of a large number of small and inexpensive sensor nodes deployed in the monitoring area collect and process the information and then send the information to the observer [1]. Localization is an integral part of WSN and the application area includes but not limited to military, environmental, home and office automation, human health monitoring, tracking doctors and patients inside a hospital, etc [2] [3].

Localization algorithms in WSN can be broadly categorized as: range-based and range-free localizations according to whether the distance measurement is needed in the localization process [4]. Some popular range-based methods are received signal strength indicator (RSSI), angle of arrival (AOA), time of arrival (TOA) methods, etc [5]. TOA and AOA based methods require sensors to be equipped with extra hardware like the directional antenna, clock for time synchronization, etc [6]. The range-free localization methods estimate the location of unknown RF emitters by the connectivity and hop values of the network. The commonly known range-free techniques are distance vector hop count [7], weighted centroid method [8], etc. The range-free techniques are cost-efficient because they do not require any special hardware.

Existing 3D localization algorithms have shortcomings, such as high complexity and low positioning accuracy. Deep learning can benefit from its data-driven structure and avoid complex computations (which is common in conventional

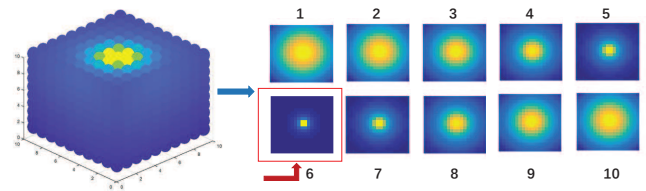


Fig. 1. The measurement data of the three-dimensional sensing network are converted into a series of two-dimensional image slices. In the $10 \times 10 \times 10 \text{ m}^3$ space, the coordinate of the RF emitter is (5,5,6). Along the height direction (z-axis), the sensor nodes are evenly arranged every 1 meter. Then, the measured values of the sensor nodes in each layer are converted to the corresponding images for display.

signal processing methods), such that the application of deep learning in signal processing in complex environments has become a trend [9]–[11]. We convert the three-dimensional sensing data into a series of two-dimensional image slices for deep learning as shown in Fig. 1. As we can see from Fig. 1, the closer it is to the RF emitters, the smaller the area of light in the slice diagram will be, and vice versa. The background is shown in dark blue. Based on this fact, in this paper, we develop a three-dimensional localization scheme of RF emitters which combines collaborative spectrum sensing with semantic segmentation. Our works of this paper are summarized as follows:

- We develop a three-dimensional localization scheme of RF emitters using a deep learning network. The localization scheme consists of three phases: the off-line training, on-line deployment and localization algorithm perform. In the off-line training phase, two-dimensional spectrum maps of RF emitters in different location coordinates are used for training. In the on-line deployment phase, the trained semantic segmentation network identify RF emitters. In the localization algorithm perform phase, a weighted localization algorithm is used for location estimation.
- We propose a semantic segmentation approach to identify

the coverage range of the RF emitters. We convert the three-dimensional sensing data into a series of two-dimensional image slices for deep learning. Then, the trained semantic segmentation network is used to identify the area covered by the RF emitters in each slice, which is used for subsequent analysis and processing.

- We design a weighted localization algorithm. For each slices after the semantic segmentation network, we calculate the value of the area covered by the RF emitters. Based on area value of each slices and their corresponding position, a weighted localization analysis algorithm is used for effective coordinate estimation.

II. SYSTEM MODEL

In order to locate the RF emitters in a specific region, we deploy the sensor nodes uniformly in the three-dimensional region of interest, as show in Fig. 2. In the wireless sensing network, sensor nodes use the energy detection. At a sensing slot, sensors measure spectrum synchronously, and transmit the local observations to a fusion center (FC), at which the data is analyzed to locate RF emitters.

In this article, we assume the received signal power at a sensor is given by the following propagation model:

$$P_{ir} = P_t \times d_i^{-\gamma} (mW), i = 1, \dots, N, \quad (1)$$

where P_t denotes the transmit power of RF emitters; d_i denotes the distance between the RF emitters and the i th sensor; γ denotes the path loss exponent; N denotes the number of sensors. In this paper, the path loss exponent γ is set to 2.

At the t -th sensing slot, the n -th sample value of the i -th sensor is

$$y_i(n, t) = \sqrt{P_{ri}} x_i(n, t) + n_i(n, t), n = 1, \dots, M, \quad (2)$$

where P_{ri} denotes the received power of the i -th sensor, M is the total sample number, $x_i(n, t)$ denotes the signal transmitted by the RF emitters. Here, $x_i(n, t)$ follows the independent and identically distribution (i.i.d.) with zero mean and unit variance [12]. In addition, $n_i(n, t)$ is modeled as i.i.d. Gaussian distribution with zero mean and variance σ_n^2 [13].

For each sensor, we consider energy detection as the means of signal detection. The test statistic for energy-based opportunity detection by each sensor is:

$$E_i(k) = \frac{1}{M} \sum_{n=1}^M [y_i(n, k)]^2. \quad (3)$$

According to the central limit theorem (CLT), when the sample number is sufficiently large (e.g., $M \gg 10$), $E_i(k)$ can be approximated by a Gaussian random variable with [14]:

$$E_i(k) \sim \mathcal{N}(\mu_1, \sigma_1^2), \quad (4)$$

where $\mu_1 = (1 + \gamma_{1i}) \sigma_n^2$, $\sigma_1^2 = 2(1 + 2\gamma_{1i}) \sigma_n^4 / M$. $\gamma_{1i} = P_{ri} / \sigma_n^2$ represents the received signal-to-noise ratio (SNR) of the i -th sensor.

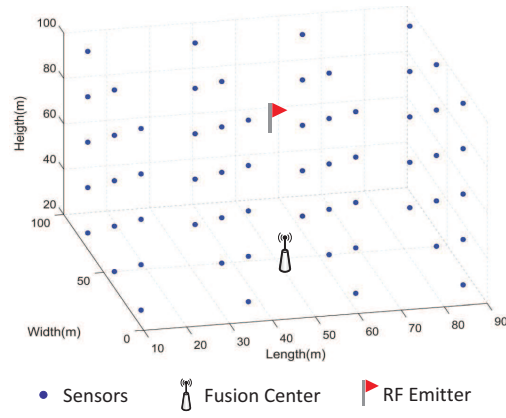


Fig. 2. Sensor nodes are deployed uniformly in the three-dimensional region of interest. As show in the picture, $3 \times 4 \times 5$ sensors uniformly arrange in the $100 \times 100 \times 100 \text{ m}^3$ space.

III. PROPOSED LOCALIZATION SCHEME

We develop a three-dimensional localization scheme of RF emitters using a semantic segmentation network, as show in Fig. 3. The localization system consists of three phases: the off-line training, on-line deployment and localization algorithm perform.

A. Model Training

Semantic segmentation is a basic task in computer vision. Semantic segmentation is to do intensive segmentation of the image, segmentation each pixel to the specified category. In this article, we use the Deeplab V3 network [15] to identify the area covered by the RF emitters. The Deeplab V3 networks use space pyramid pooling module (SPP) and encoding and decoding structure for semantic segmentation of deep network structure. SPP uses different resolution features of multiple proportions and multiple effective sensing fields to mine multi-scale context content information and gradually reconstruct spatial information of encoding and decoding structures to better capture object boundaries.

The training data are obtained by simulation. In each simulation, a random coordinate of a RF emitter in two-dimensional is generated and the corresponding two-dimensional sensing data are converted into an image called spectrum map. Then, Labelme tool is used to label the coverage area of RF emitters in the spectrum maps. The labeled images are input to the network for training. During the training, the network is expected to segmentation each pixel to the specified category.

B. Semantic Segmentation Approach

Sensors in WSN measure spectrum synchronously, and transmit local observations to a fusion center. It is difficult to process 3D sensing data directly, so we convert the three-dimensional sensing data into a series of two-dimensional image slices according to the location of each sensor. Based on the fact that the closer it is to the RF emitters, the smaller the area of light in the slices will be, we need to find the slices with a smaller light area to locate RF emitters. The trained

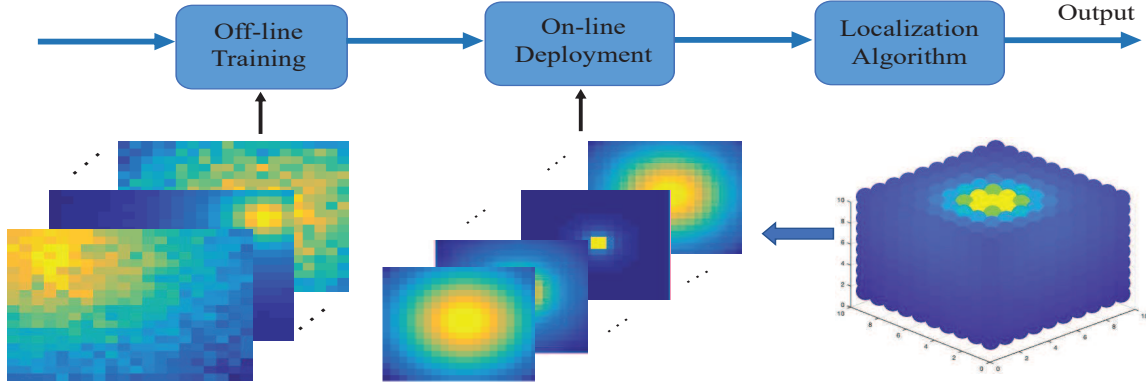


Fig. 3. The three-dimensional localization scheme.

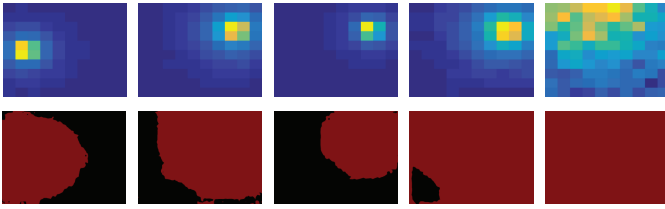


Fig. 4. The recognition results of semantic segmentation network. The images in second row are the recognition result of the first row after semantic segmentation, in which the dark blue background is shown as black and the coverage area of RF emitters is shown as red.

semantic segmentation network identifies the coverage range of the RF emitters which is assigned the value of 1, and the dark blue background is assigned the value of 0, as show in Fig. 4. Then, we can obtain the coverage area of RF emitters by calculating the sum of the number 1 in each slice.

C. Localization Algorithm

As we can see from Fig. 1, the closer it is to the RF emitters, the smaller the area of light in the slice diagram will be, and vice versa. It can be inferred that the location of RF emitter is between the corresponding positions of the two slices with the minimum coverage area of the RF emitters. For precise localization, we design a weighted localization algorithm, and the procedure of this localization algorithm is summarized in algorithm 1. We represent the process of converting the three-dimensional sensing data into images along the x, y, and z axes as the variable i from 1 to 3.

IV. SIMULATIONS

We consider a $100 \times 100 \times 100 \text{ m}^3$ space, and the sensors are placed uniformly within it. The simulation results are the average of 100 experiments under the same conditions. The root-mean-square error (RMSE) for localization is defined as

$$RMSE = \sqrt{\frac{1}{C} \sum_{c=1}^C ((\hat{x}_c - x_0)^2 + (\hat{y}_c - y_0)^2 + (\hat{z}_c - z_0)^2)}, \quad (5)$$

Algorithm 1 Localization Algorithm

Input: Three-dimensional sensing data and coordinates of each sensor.

- 1: **for** $i \in [1, 3]$ **do**
- 2: Convert three-dimensional sensing data into a series of image slices according to the location of each sensor;
- 3: Input the slices into the trained semantic segmentation network to get identification result images;
- 4: Calculate the area covered by the RF emitter in each slice according to the identification result images;
- 5: Find the two smallest area values in the slices S_{i1}, S_{i2} ($S_{i1} < S_{i2}$), and the corresponding coordinate positions $\hat{P}_{i1}, \hat{P}_{i2}$;
- 6: Set the threshold ε ;
- 7: **if** $S_2 > \varepsilon$ **then**
- 8: $P_i = \hat{P}_{i1}$
- 9: **else**
- 10: $P_i = \frac{S_{i1} * \hat{P}_{i2}}{S_{i1} + S_{i2}} + \frac{S_{i2} * \hat{P}_{i1}}{S_{i1} + S_{i2}}$
- 11: **end if**
- 12: **end for**

Output: Coordinates of RF emitter $P = [P_1, P_2, P_3]$.

where $[x_0, y_0, z_0]$ is the coordinates of the RF emitter, C is the number of Monte-Carlo experiments.

A. Experimental Setup

Keras, a widely used deep learning framework, is utilized to build semantic segmentation network-based model for localization. The Deeplab V3 network is trained as follows: 1) the signals received from sensors are obtained from computer simulations and the sampling number M is 100; 2) the coverage area of RF emitter in each picture is manually marked with the Labelme tool; 3) 4000 two-dimensional spectrum maps of different location coordinates of RF emitter are collected to form training sets; 4) data sets are fed to deep learning networks for training with Keras; 5) after a maximum of 3000 training iterations, the trained models can be obtained. In this paper, training is conducted on our computing server with a

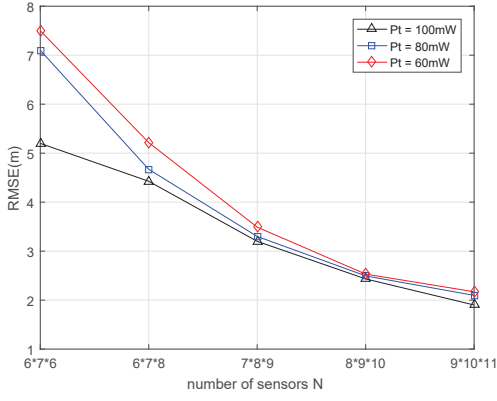


Fig. 5. Impact of the number of sensors on localization accuracy at different signal transmission power. Here, the noise power σ_n^2 is 0.01 mW and the sample number is $M = 100$.

Nvidia GTX 1080 GPU. After training, test sets are fed to the semantic segmentation network for pixel classification. The weighted localization algorithm processes and analyzes the images after semantic segmentation for RF emitters coordinate estimate.

B. Impact of The Number of Sensor Nodes

The more sensors in the wireless sensing network, the more information can be obtained and the number of different sensor nodes corresponds to different resolution of the image. Thus, the number of sensor nodes in wireless sensing network is a key parameter. In each case, we set the noise power σ_n^2 as 0.01 mW. Fig. 5 demonstrates the impact of the number of sensors at different signal transmission power on the localization accuracy. The number of sensors $6 \times 7 \times 8$ denotes the number of sensors parallel to the x, y and z axes is 6, 7, and 8, respectively. As shown in this figure, higher number of sensors incurs a better localization accuracy.

C. Impact of The Signal Transmission Power

In the wireless sensor network, the SNR of each sensor is different. Therefore, we explore the effect of different signal transmission power on localization performance. As shown in the Fig. 6, a higher signal transmission power incurs a better localization accuracy.

D. Accuracy Comparisons

We extend the classical weighted centroid localization algorithm to three-dimensional space and compare it with the proposed algorithm at different transmission power of RF emitters. As we can see in Fig. 7, the localization performance of the proposed algorithm are both better than three-dimensional weighted centroid localization algorithm at different number of sensors.

E. The Extended Weighted Centroid Localization Algorithm

In order to compare with the proposed algorithm, we extend the classical weighted centroid localization algorithm [8] to three-dimensional space. In the three-dimensional space, the

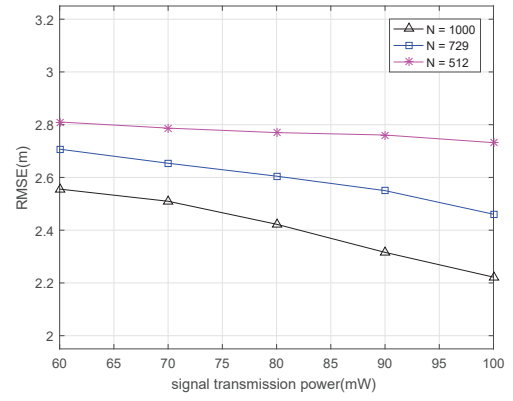


Fig. 6. Impact of the signal transmission power on localization accuracy at different number of sensors. Here, the noise power σ_n^2 is 0.01 mW and the sample number is $M = 100$.

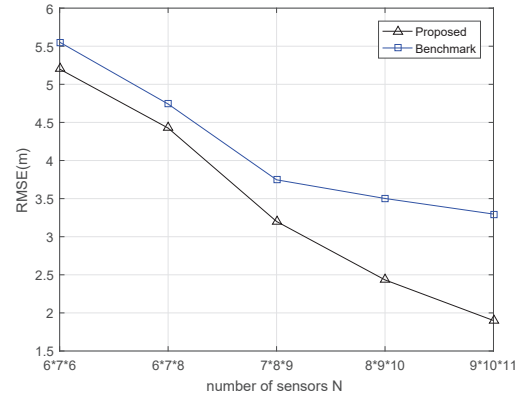


Fig. 7. Accuracy comparisons between proposed and benchmark method at different number of sensors. Different number of sensors paralleled to the x, y, and z axes are deployed. Here, the noise power σ_n^2 is 0.01 mW, the sample number is $M = 100$ and signal transmission power $P_t = 100$ mW.

intersection of two circles is extended to the intersection of three spherical surface at two points, using the tetrahedral measurement method for positioning.

The three spheres are determined by the RSSI of the RF emitter S received at three sensors A , B and C . The corresponding radii are $d_1 = \hat{L}_{AS}$, $d_2 = \hat{L}_{BS}$, $d_3 = \hat{L}_{CS}$. Two possible positions of the RF emitter can be estimated: S_1 and S_2 . According to the RSSI received at the fourth sensors D , we can obtain the radius is $d_4 = \hat{L}_{DS}$. Compare the value of $|\hat{L}_{DS} - \hat{L}_{DS1}| / \hat{L}_{DS1}$ and $|\hat{L}_{DS} - \hat{L}_{DS2}| / \hat{L}_{DS2}$ and select the smaller one of S_1 and S_2 as the approximate position of the RF emitter S , denoted as (x_1, y_1, z_1) . Similarly, considering the other three cases, we will derive the other three approximate positions (x_2, y_2, z_2) , (x_3, y_3, z_3) , (x_4, y_4, z_4) . Take the weighted center of mass of these four points, and we can derive the approximate position of S .

The weighted centroid are:

$$\begin{aligned}\hat{x} &= \frac{\frac{x_1}{d_1+d_2+d_3} + \frac{x_2}{d_1+d_4+d_3} + \frac{x_3}{d_1+d_2+d_4} + \frac{x_4}{d_4+d_2+d_3}}{\frac{1}{d_1+d_2+d_3} + \frac{1}{d_1+d_4+d_3} + \frac{1}{d_1+d_2+d_4} + \frac{1}{d_4+d_2+d_3}}, \\ \hat{y} &= \frac{\frac{y_1}{d_1+d_2+d_3} + \frac{y_2}{d_1+d_4+d_3} + \frac{y_3}{d_1+d_2+d_4} + \frac{y_4}{d_4+d_2+d_3}}{\frac{1}{d_1+d_2+d_3} + \frac{1}{d_1+d_4+d_3} + \frac{1}{d_1+d_2+d_4} + \frac{1}{d_4+d_2+d_3}}, \\ \hat{z} &= \frac{\frac{z_1}{d_1+d_2+d_3} + \frac{z_2}{d_1+d_4+d_3} + \frac{z_3}{d_1+d_2+d_4} + \frac{z_4}{d_4+d_2+d_3}}{\frac{1}{d_1+d_2+d_3} + \frac{1}{d_1+d_4+d_3} + \frac{1}{d_1+d_2+d_4} + \frac{1}{d_4+d_2+d_3}}.\end{aligned}\quad (6)$$

When there are m sensing data, C_m^4 tetrahedrons can be formed, and each tetrahedron generates an approximate coordinate of the RF emitter. The final estimated position of the RF emitter \hat{S} can be obtained by using the centroid algorithm again.

The algorithm processes are described as follows:

- 1) Sort the received RSSI values from large to small. Select the first K large values and the coordinates of the corresponding sensors;
- 2) Estimate coordinate of RF emitter:
 - I Select all four points in the set that can make up the tetrahedron to form tetrahedron-set;
 - II For any tetrahedron $(c_{ii}, c_{jj}, c_{kk}, c_{ll})$ in tetrahedron-set, perform the weighted centroid algorithm to obtain an approximate set of RF emitter coordinates: $\{k_1, k_2, k_3, \dots, k_p\}$;
 - III Perform the weighted centroid method again for the approximate coordinate set as follows:

$$\begin{aligned}b &= \sum_{i=1}^p \frac{1}{d_{1,i} + d_{2,k_i} + d_{3,k_i} + d_{4,k_i}}, \\ x &= \frac{\sum_{i=1}^p \frac{\hat{x}_{k_i}}{d_{1,i} + d_{2,k_i} + d_{3,k_i} + d_{4,k_i}}}{b}, \\ y &= \frac{\sum_{i=1}^p \frac{\hat{y}_{k_i}}{d_{1,i} + d_{2,k_i} + d_{3,k_i} + d_{4,k_i}}}{b}, \\ z &= \frac{\sum_{i=1}^p \frac{\hat{z}_{k_i}}{d_{1,i} + d_{2,k_i} + d_{3,k_i} + d_{4,k_i}}}{b},\end{aligned}\quad (7)$$

where $(d_{1k_i}, d_{2k_i}, d_{3k_i}, d_{4k_i})$ denotes the distance from $(c_{ii}, c_{jj}, c_{kk}, c_{ll})$ to the RF emitter S ;

- 3) If the tetrahedron that meets the condition cannot be found, then the coordinate of RF emitter can be calculated by $x = \frac{\sum_{i=1}^K Q_i x_i}{\sum_{i=1}^K Q_i}$, $y = \frac{\sum_{i=1}^K Q_i y_i}{\sum_{i=1}^K Q_i}$, $z = \frac{\sum_{i=1}^K Q_i z_i}{\sum_{i=1}^K Q_i}$, where $Q_i = \frac{K \times R_i}{\sum_{i=1}^K R_i}$, and R_i is the RSSI of each sensor.

V. CONCLUSION

In this paper, we have developed a three-dimensional localization scheme of RF emitters using semantic segmentation network. We convert the three-dimensional sensing data into a series of two-dimensional image slices for deep learning. For precise localizing, a weighted localization algorithm has been proposed. The simulation results verified the detection

performances in terms of the number of sensors and signal transmitting power.

ACKNOWLEDGMENT

This work is supported by the National Natural Science Foundation of China (No. 61801216, No. 61871398, No. 61931011, No. 61631020), the Natural Science Foundation for Distinguished Young Scholars of Jiangsu Province (No. BK20190030), the Natural Science Foundation of Jiangsu Province (No. BK20180420), the open research fund of Key Laboratory of Dynamic Cognitive System of Electromagnetic Spectrum Space (Nanjing Univ. Aeronaut. Astronaut.), Ministry of Industry and Information Technology, Nanjing, 211106, China (No. KF20181913).

REFERENCES

- [1] K. F. Navarro and E. Lawrence, "Wsn applications in personal healthcare monitoring systems: A heterogeneous framework," in *2010 Second International Conference on eHealth, Telemedicine, and Social Medicine*, 2010, pp. 77–83.
- [2] K. F. Navarro and E. Lawrence, "WSN applications in personal healthcare monitoring systems: A heterogeneous framework," in *Second International Conference on Ehealth*, 2010.
- [3] L. Gavrilovska, S. Krco, V. Milutinovi, I. Stojmenovic, and R. Trobec, "Application and multidisciplinary aspects of wireless sensor networks concepts, integration, and case studies," *Computer Communications & Networks*, vol. 127, no. 4, pp. 407–421, 2010.
- [4] K. Langendoen and N. Reijers, "Distributed localization in wireless sensor networks: a quantitative comparison," *Computer Networks*, vol. 43, no. 4, pp. 499–518, 2003.
- [5] G. Han, J. Jiang, C. Zhang, T. Q. Duong, M. Guizani, and G. K. Karagiannidis, "A survey on mobile anchor node assisted localization in wireless sensor networks," *IEEE Communications Surveys & Tutorials*, vol. 18, no. 3, pp. 2220–2243, 2016.
- [6] J. Kumari, P. Kumar, and S. K. Singh, "Localization in three-dimensional wireless sensor networks: a survey," *Journal of Supercomputing*, 2019.
- [7] Y. Xu, Y. Zhuang, and J. J. Gu, "An improved 3D localization algorithm for the wireless sensor network," *International Journal of Distributed Sensor Networks*, vol. 2015, pp. 1–9, 2015.
- [8] W. Chen, W. Li, H. Shou, and B. Yuan, "Weighted centroid localization algorithm based on RSSI for wireless sensor networks," *Journal of Wuhan University of Technology*, no. 2, pp. 81–84, 2006.
- [9] H. Sun, X. Chen, Q. Shi, M. Hong, X. Fu, and N. D. Sidiropoulos, "Learning to optimize: Training deep neural networks for interference management," *IEEE Transactions on Signal Processing*, vol. 66, no. 20, pp. 5438–5453, 2018.
- [10] B. Wu, K. Li, F. Ge, Z. Huang, M. Yang, S. M. Siniscalchi, and C. Lee, "An end-to-end deep learning approach to simultaneous speech dereverberation and acoustic modeling for robust speech recognition," *IEEE Journal of Selected Topics in Signal Processing*, vol. 11, no. 8, pp. 1289–1300, 2017.
- [11] J. Zhu, T. Park, P. Isola, and A. A. Efros, "Unpaired image-to-image translation using cycle-consistent adversarial networks," in *2017 IEEE International Conference on Computer Vision (ICCV)*, 2017, pp. 2242–2251.
- [12] C. Chen, H. Cheng, and Y. Yao, "Cooperative spectrum sensing in cognitive radio networks in the presence of the primary user emulation attack," *IEEE Transactions on Wireless Communications*, vol. 10, no. 7, pp. 2135–2141, 2011.
- [13] G. Ding, Q. Wu, Y. Yao, J. Wang, and Y. Chen, "Kernel-based learning for statistical signal processing in cognitive radio networks: Theoretical foundations, example applications, and future directions," *IEEE Signal Processing Magazine*, vol. 30, no. 4, pp. 126–136, 2013.
- [14] H. Utkowitz, "Energy detection of unknown deterministic signals," *Proceedings of the IEEE*, vol. 55, no. 4, pp. 523–531, 1967.
- [15] V. Badrinarayanan, A. Kendall, and R. Cipolla, "Segnet: A deep convolutional encoder-decoder architecture for image segmentation," *IEEE Transactions on Pattern Analysis and Machine Intelligence*, vol. 39, no. 12, pp. 2481–2495, 2017.